Bout-based Gas Source Localization using Aerial Robot Swarms

Felix Häusler, Jan Stührenberg*, and Kay Smarsly
Hamburg University of Technology
Hamburg, Germany
*jan.stuehrenberg@tuhh.de

Patrick P. Neumann*
Federal Institute for Materials Research and Testing (BAM)
Berlin, Germany
*patrick.neumann@bam.de

***Abstract*—Gas source localization (GSL) helps mitigate the impact of industrial accidents and natural disasters. While GSL may be dangerous and time-consuming when performed by humans, swarms of agile and inexpensive nano aerial robots may increase the safety and efficiency of gas source localizations. Since the small payloads of nano aerial robots limit the sensing and computing resources, strategies adapted from biological swarms, such as colonies of social insects, are used to coordinate robot swarms. Most swarm GSL strategies are based on the assumption that the maxima of gas concentrations are sufficiently close to the gas sources. However, prior studies have indicated that the occurrence of "bouts", a metric for the intermittency of gas distributions, may advantageously be used as a more accurate gas source proximity indicator. This paper presents a swarm GSL strategy employing bouts as source proximity indicators and a bio-inspired pheromone system for communication. Nano aerial robots, deployed in this study, act as agents and emit pheromone markers in an artificial environment upon detecting bouts. Leveraging the concept of artificial potential fields, the agents switch between exploiting the knowledge of the swarm by following pheromone gradients and exploring the search space by targeting a random point. The agents are repelled by each other and by walls to avoid collisions. The swarm GSL strategy is implemented into three nano aerial robots and validated in a real-world experiment in an indoor environment with a single gas source. The results indicate that the the swarm GSL strategy presented in this paper is capable of GSL in indoor environments and that the intermittency of gas distributions is a better source proximity indicator than the mean concentration.**

***Index Terms*—Mobile robotic olfaction; nano aerial robot; gas source localization; bouts; distributed robotics**

I. Introduction

Gas source localization (GSL) using mobile robots is of value in a range of industrial, environmental, and humanitarian tasks, where the search space is dangerous and/or hard to reach. Using multiple robots may increase the search efficiency, but require reliable coordination. Biological swarms, such as populations of social insects, are a popular source of inspiration to achieve reliable coordination between large numbers of relatively simple agents. In the field of mobile robot olfaction (MRO), most swarm-inspired research treats GSL as a concentration optimization problem based on the assumption that the gas concentration maximum is close to the true source location [1]. Under this assumption, existing swarm intelligence algorithms may be used for GSL. The most popular algorithms are particle swarm optimization (PSO) and ant colony optimization (ACO) [2]. While PSO and ACO are validated for many use cases, PSO and ACO generally do not consider the physical and dynamic aspects of the real world. It is believed that taking direct inspiration from biological swarms could lead to simpler, yet more efficient algorithms, as biological swarms operate under similar conditions as robotic swarms. Furthermore, several studies have demonstrated that the concentration maximum is not necessarily a good source proximity indicator in complex environments, and that the intermittency of the gas plume, measured through so-called bouts, could be a better choice [3].

The key contribution of this work is the introduction of a swarm GSL strategy that uses bouts as a proximity indicator and swarm-inspired pheromone communication (Sec. II) and its validation in simulations and real-world experiments (Sec. III): Agents detect bouts and emit artificial pheromones that, once integrated into a map, are used for navigation and collision avoidance. Exploration-exploitation balance is achieved by occasionally ignoring the pheromone map. The highest pheromone concentration indicates the source estimation. Although not being the first strategy using pheromone communication [4], our approach integrates, stores, and diffuses the pheromone signals, making it scalable, robust to noise and defects, reactive to changes in source position, and simplifies the agents to being purely reactive.

II. Bout-based swarm GSL strategy

The strategy proposed in this paper consists of two parts, (i) the artificial environment (Sec. II-A), which coordinates the swarm, and (ii) the agents (Sec. II-B), which collect measurements and release pheromones into the artificial environment when bouts are detected. The following subsections present both parts and their interactions.

A. Artificial Environment

The purpose of the artificial environment is to enable the agents to effectively collaborate. The artificial environment is implemented through the artificial potential field (APF) concept [5]. Upon request, the agents receive the attractive force of the artificial pheromone map (APM) and the repulsive force of the anti-collision layer. The APM mimics the environmental part in biological pheromone communication. The APM allows (i) integrating an arbitrary number of signals into a function of space and (ii) diffusing the function over time. The

first aspect allows an arbitrary number of simplistic organisms to collaborate without being aware of each other, and the second aspect allows the system to work probabilistically, as the effect of individual markers will fade into the background if not reinforced.

The APM is represented by a discrete map, with agents releasing pheromone markers – particles of predefined size and intensity – at their current position. A diffusing kernel is applied to the map every time a new pheromone marker is deposited, to avoid losing information if no new pheromones are deposited and to weight newer entries higher than preceding ones. To calculate the attractive force, a kernel-smoothed copy of the APM is converted into an APF. Here, the kernel size regulates the range of influence of the pheromone markers. Next, the gradient or force of the APF is computed and vortexed according to the following expression:

$$F_{vortex,x} = F_x + F_y \cdot \gamma, \tag{1a}$$

$$F_{vortex,y} = F_y - F_x \cdot \gamma, \tag{1b}$$

where $F_{vortex,x/y}$ denotes the resulting vortexed force, $F_{x/y}$ representss the initial force in x/y direction, and γ is a factor determining vorticity and spin direction. Vortexation causes agents to circle promising areas instead of heading straight to a pheromone peak, helping the agents to avoid local optima. The vortexed force field is lastly normalized to $[0, 1]$, which is important to ensure collision avoidance. Upon an agent requesting the forces at its position, the resulting force field and the repulsive force is returned.

To avoid collisions, a repulsive force F_{rep} is calculated for each agent based on the distance to obstacles and other agents using an adaption of the FIRAS function presented in [5]:

$$F_{rep} = \begin{cases} \left(\frac{d_{min}^2}{\frac{1}{d_{min}} - \frac{1}{d_{max}}} \right) \left(\frac{1}{d} - \frac{1}{d_{max}} \right) \frac{1}{d^2} & \text{, if } d \leq d_{max} \\ 0 & \text{, otherwise} \end{cases} \tag{2}$$

where d represents the distance between the requesting agent and the obstacle, and d_{min} and d_{max} represent parameters for the closest distance allowed and the range of influence of the obstacle, respectively. Both parameters are chosen based on the positioning accuracy and the distance the agents can safely pass each other. For optimal navigation, APM and anti-collision forces should have the same spin direction, requiring a reverse rotation for the enclosing wall repulsion forces. The rotation helps avoid deadlocks during obstacle avoidance.

B. Agents

The agents are modeled as reactive particles with a bout detector and motion controller. The bout detector is adapted from [6]: The agents monitor the second derivative of the concentration signal for a positive zero crossing, which is referred to as a bout. A bout indicates that a sensor is in contact with a new plume filament. Noise-induced bouts are filtered by a threshold, while bouts that do not exceed a threshold are discarded. The raw signal and both derivatives are smoothed with an exponentially weighted moving average filter before further processing. The positions of accepted bouts are sent to the artificial environment, which integrates the bouts as pheromone markers into the APM.

The motion controller navigates the agents, which either follow the attractive force of the APM to exploit swarm knowledge or the attractive force of a randomly generated setpoint to explore the search space. The attractive force of the random setpoint $\vec{F}_{set}$ is defined by:

$$\vec{F}_{set} = \begin{cases} \frac{\vec{X}_{set} - \vec{X}_{pos}}{\left\| \vec{X}_{set} - \vec{X}_{pos} \right\|} & \text{, if } \left\| \vec{X}_{set} - \vec{X}_{pos} \right\| > \varepsilon \\ \frac{\vec{X}_{set} - \vec{X}_{pos}}{\varepsilon} & \text{, otherwise} \end{cases} \tag{3}$$

$\vec{X}_{pos}$ and $\vec{X}_{set}$ are the position vectors of the agent and setpoint, respectively, and ε is the distance in which the agent slows down linearly. Then, the resultant force is normalized and factored by the maximum linear velocity to obtain the velocity vector, which is passed to the low-level controller of the aerial robot.

III. Implementation and Validation

The swarm used for validation consists of palm-sized Crazyflie 2.0 quadrocopters (Bitcraze AB, [7]) equipped with a 3D local positioning system and a custom-build sensor deck comprising an optical motion detection system and two SGP30 metal-oxide semiconductor gas sensors (Sensirion, [8]) [9]. The bouts are detected from the transient signals of the ethanol pixel of the gas sensors. A quadrocopter weighs $\approx 39.6\,\mathrm{g}$ and achieves flight times of up to 5 minutes. The strategy proposed in this paper is implemented via the Crazyswarm Python API [10] and the Robot Operating System (ROS). The strategy is validated in simulations (Sec. III-A) and in real-world experiments (Sec. III-B).

A. Simulation

The source proximity indication potential of bouts was validated in simulations using GADEN [11], a simulation framework designed for algorithms in the field of MRO. In a simulated environment, 12 agents were deployed in a $(6 \times 10)\,\mathrm{m}^2$ room with two openings, one of which served as the inlet and the other as the outlet, containing a single gas source placed at $(3.0, 1.5, 0.75)\,\mathrm{m}$. The pre-calculated wind

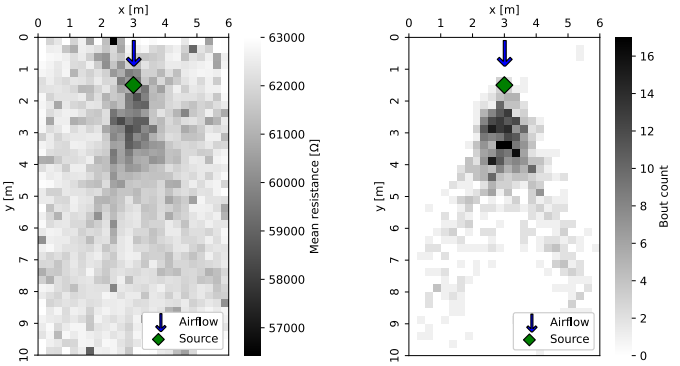

(a) Mean readings (b) Total bout counts

Fig. 1. Maps of the simulated sensor data.

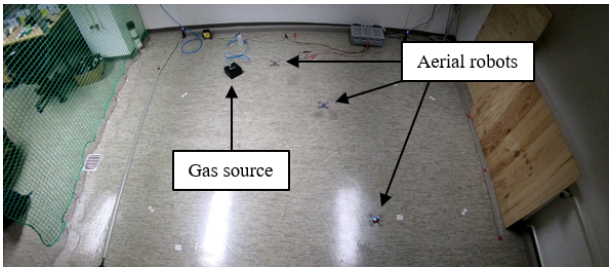

Fig. 2. Real-world experiments.

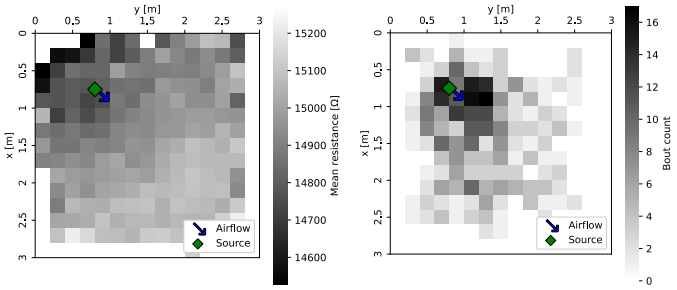

(a) Mean readings (b) Total bout counts

Fig. 3. Maps of the real-world sensor data.

field provided by GADEN consisting of strong, fluctuating airflow was used. Agents randomly traversed the room at a height of $0.5\,\mathrm{m}$, logging sensor measurements and positions at $10\,\mathrm{Hz}$. The simulation ran for $30\,\mathrm{min}$ with 10x acceleration.

Approximately 180,000 sensor readings were recorded during the simulation. Fig. 1(a) shows the mean sensor readings (lower resistances correspond to higher concentrations) and Fig. 1(b) shows the total bout count per cell, both visualized in discrete maps of the search space. Both maps show a clustering of cells with low resistances and high bout counts, respectively, close to the source, albeit offset $1.5\,\mathrm{m}$ in the direction of airflow. While the gradients in Fig. 1(a) are relatively smooth and no boundaries are visible, the clusters in Fig. 1(b) show a denser V-shaped distribution with steep gradients in downwind direction. The simulation results suggest that the bout count can be a more accurate and less noisy source proximity indicator than the mean concentration.

B. Real-World Experiments

The swarm GSL strategy is validated in real-world experiments. A swarm of three aerial robots is deployed in a cuboid indoor environment with a 2D search space of approx. $(3 \times 3)\,\mathrm{m}^2$ containing a single gas source, as shown in Fig. 2. The gas source, consisting of a tube connected to a bottle of liquid ethanol and a $1\,\mathrm{W}$ fan, was positioned at $(0.80, 0.75)\,\mathrm{m}$ and elevated $0.1\,\mathrm{m}$ off the ground. Pressurized air was introduced to stimulate evaporation, and the emission rate was indirectly controlled by setting the airflow to $2\,\mathrm{l/min}$. The source was rotated to face the center of the search space and opened roughly 1 minute before each run. Between the runs, the source was closed and the room was ventilated for comparable starting conditions. The robots terminated each run either by landing/crashing or running out of battery. Parameters required by the algorithm were chosen heuristically and data was logged at $10\,\mathrm{Hz}$.

During 16 runs, approximately 20,000 measurements were recorded. The individual flight times were in a range from $0\,\mathrm{s}$ (crash at takeoff) to $329\,\mathrm{s}$, and the combined flight times of all three aerial robots were in the range between $303\,\mathrm{s}$ and $903\,\mathrm{s}$ with a mean of $613.4\,\mathrm{s} \pm 165.2\,\mathrm{s}$. The experimental results are shown in Figs. 3 and 4. The mean resistance plot in Fig. 3(a) shows smooth gradients, similar to Fig. 1(a). However, in contrast to Fig. 1(a), the cluster of low mean resistance is shifted in upwind direction. The bout distributions in Fig. 3(b), again, show dense clusters with steep gradients, but in contrast to the simulation results, no V-shape is visible. Fig. 4(a) shows the final source location estimates. All estimation errors are in airflow direction. Furthermore, the mean error is close to the center line of the airflow of the fan. Fig. 4(b) shows the average estimation error of the combined flight time scaled by the number of active agents, including the results of each individual run. The source estimation, on average, improves rapidly during the first $90\,\mathrm{s}$ combined flight time. After $330\,\mathrm{s}$, the final source estimation error is on average $0.7\,\mathrm{m} \pm 0.29\,\mathrm{m}$ ranging from $0.25\,\mathrm{m}$ (run #10) and $1.28\,\mathrm{m}$ (run #8), and improves after $540\,\mathrm{s}$ to $0.6\,\mathrm{m} \pm 0.21\,\mathrm{m}$.

IV. Conclusions and Future Work

In this paper, a swarm GSL strategy using bouts as source proximity indicators and virtual pheromones as communication medium was introduced. Simulations and real-world experiments demonstrated that bouts may be strong source proximity indicators in indoor environments compared to using mean concentrations. Furthermore, the strategy proposed in this paper has shown promising results in real-world experiments, although still in its infancy. Potential future work may focus on tuning the parameter set of the swarm GSL strategy. Further improvements may be achieved by introducing wind information and extending the strategy to three dimensions. Furthermore, the swarm GSL strategy may be compared to existing algorithms under identical environmental conditions.

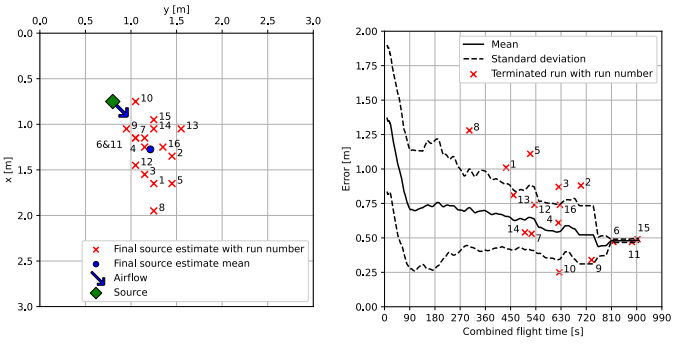

(a) (b)

Fig. 4. Experimental results: (a) Final estimations in space and (b) smoothed mean error of combined flight time of the experiments with standard deviation over time. Run time individually scaled by the number of active agents, and estimations excluded after termination.

REFERENCES

[1] T. Jing, Q.-H. Meng, and H. Ishida, "Recent progress and trend of robot odor source localization," *IEEJ Transactions on Electrical and Electronic Engineering*, vol. 16, no. 7, pp. 938–953, 2021.

[2] J. Wang, Y. Lin, R. Liu, and J. Fu, "Odor source localization of multi-robots with swarm intelligence algorithms: A review," *Frontiers in Neurorobotics*, vol. 16, 2022.

[3] M. Schmuker, V. Bahr, and R. Huerta, "Exploiting plume structure to decode gas source distance using metal-oxide gas sensors," *Sensors and Actuators B: Chemical*, vol. 235, pp. 636–646, 2016.

[4] Q.-H. Meng, W.-X. Yang, Y. Wang, and M. Zeng, "Multi-robot odor-plume tracing in indoor natural airflow environments using an improved aco algorithm," in *Proc. 2010 IEEE International Conference on Robotics and Biomimetics*, 2010, pp. 110–115.

[5] O. Khatib, "Real-time obstacle avoidance for manipulators and mobile robots," in *Proc. 1985 IEEE International Conference on Robotics and Automation*, St. Louis, MO, USA, 1985, pp. 500–505.

[6] J. Burgués, V. Hernández, A. J. Lilienthal, and S. Marco, "Smelling nano aerial vehicle for gas source localization and mapping," *Sensors*, vol. 19, no. 3, 2019.

[7] Bitcraze AB, "Crazyflie 2.0," accessed: May 9, 2023. [Online]. Available: https://www.bitcraze.io/products/old-products/crazyflie-2-0/

[8] Sensirion AG, "Datasheet SGP30 – Sensirion Gas Platform," May 2020, accessed: May 9, 2023. [Online]. Available: https://sensirion.com/media/documents/984E0DD5/61644B8B/Sensirion_Gas_Sensors_Datasheet_SGP30.pdf

[9] P. P. Neumann, P. Hirschberger, Z. Baurzhan, C. Tiebe, M. Hofmann, D. Hüllmann, and M. Bartholmai, "Indoor air quality monitoring using flying nanobots: Design and experimental study," in *Proc. 2019 IEEE International Symposium on Olfaction and Electronic Nose*, Fukuoka, Japan, 2019.

[10] J. A. Preiss, W. Honig, G. S. Sukhatme, and N. Ayanian, "Crazyswarm: A large nano-quadcopter swarm," in *Proc. 2017 IEEE International Conference on Robotics and Automation*, Singapore, Singapore, 2017, pp. 3299–3304.

[11] J. Monroy, V. Hernandez-Bennets, H. Fan, A. Lilienthal, and J. Gonzalez-Jimenez, "Gaden: A 3d gas dispersion simulator for mobile robot olfaction in realistic environments," *Sensors*, vol. 17, no. 7, 1479, 2017.